PHYSICAL REVIEW B **66**, 041103(R) (2002)

Successive phase transitions and energy-gap formation in CeRhAs

T. Sasakawa,[1] T. Suemitsu,[1] T. Takabatake,[1] Y. Bando,[2] K. Umeo,[1] M. H. Jung,[1] M. Sera,[1] T. Suzuki,[1] T. Fujita,[1] M. Nakajima,[3] K. Iwasa,[3] M. Kohgi,[3] Ch. Paul,[4] St. Berger,[4] and E. Bauer[4]

[1]*Department of Quantum Matter, ADSM, Hiroshima University, Higashi-Hiroshima 739-8530, Japan*

[2]*Department of Electrical Engineering, Kure National College of Technology, Kure 737-8506, Japan*

[3]*Department of Physics, Tokyo Metropolitan University, Tokyo 192-0397, Japan*

[4]*Institute of Solid State Physics, Vienna University of Technology, A-1040 Wien, Austria*

(Received 10 May 2002; published 16 July 2002)

Magnetic, transport, and x-ray diffraction measurements on single-crystal CeRhAs, the so-called Kondo insulator, have revealed successive transitions at $T_1=370$, $T_2=235$, and $T_3=165$ K. Below T_1, the unit cell is doubled along the *b* and *c* axes. Thereby, the resistivity jumps upwards and magnetic susceptibility in all the directions drops. Superlattice reflections at (0,1/3,1/3) and (1/3,0,0) appear at $T<T_2$. The latter suddenly increases below T_3 where a transport gap is enhanced. These observations indicate that the gap formation is intimately related to lattice modulations.

DOI: 10.1103/PhysRevB.66.041103 PACS number(s): 75.30.Mb, 71.27.+a, 72.15.Jf

A class of rare-earth compounds containing unstable $4f$ electrons has a (pseudo) gap in heavy-electron bands at the Fermi level in the coherent ground state.[1–3] Canonical systems YbB_{12} and $Ce_3Bi_4Pt_3$ with cubic structures possess a well-defined gap of the order of the Kondo temperature. The gap formation is therefore thought to originate from the Kondo coupling between conduction electrons and localized $4f$ spins. However, an incomplete gap was observed in orthorhombic systems CeNiSn and CeRhSb, where Ce atoms form a zigzag chain along the *a* axis of the ε-TiNiSi-type structure.[2,4] Anisotropic hybridization of $4f$ wave functions with a half-filled conduction band was proposed to be responsible for the incomplete gapping.[5] Narrow pseudogaps at the Fermi level give rise to a significantly enhanced thermopower of the order of 100 μV/K at low temperatures.[6–8] For this reason, Kondo insulators or semiconductors have attracted much attention as potential thermoelectric materials.[9]

The compound CeRhAs, being isostructural to CeNiSn and CeRhSb, was first synthesized by Yoshii *et al.* in a polycrystalline form.[10] The intermediate-valence state of this compound was indicated by the weak temperature dependence of the magnetic susceptibility with a broad maximum at around 450 K. Furthermore, the electrical resistivity showed activation-type behavior with an energy gap of 144 K. This behavior contrasts with the metallic behavior in the resistivity of single crystals of CeNiSn and CeRhSb.[2] Recent studies of CeRhAs by photoemission spectroscopy[11,12] revealed the development of a gap of 50–60 meV on cooling below approximately 210 K. It was claimed that the gap magnitude for CeRhSb and CeRhAs derived from the photoemission spectra can be scaled with the Kondo temperature, $T_K=360$ K and 1200 K, respectively. Thus, CeRhAs was classified into the class of Kondo insulators where the local Kondo coupling is essential for the gap formation.

In this paper, we report the magnetic, transport, and structural properties of single-crystal CeRhAs. Our experimental results show that the gap formation in the electronic density of states is associated with periodic lattice distortions. Single-crystal samples have been grown by the Bridgman technique. Pieces of As and a premelted $CeRh_{1.02}$ ingot in the nominal stoichiomerty of 1:1.02:1 were loaded in a tungsten crucible, which was then shielded by an argon-arc welder. The crucible was heated to 1650 °C and cooled slowly to grow a single crystal. The samples obtained at the bottom of the crucible were characterized by a metallographic examination and electron-probe microanalysis. Thereby, an impurity phase of $CeRh_{1.8}As$ of less than 1% was detected. Stacking faults perpendicular to the orthorhombic *a* axis was viewed by optical microscopy. The single-crystal nature for lumps of 3 mm in diameter was verified by using Laue diffraction method.

The electrical resistivity and Hall coefficient were measured by conventional methods on bar-shaped single-crystal samples. The measurements of thermopower and thermal conductivity were done with unoriented crystals of 4 mm in length that is minimum to produce an appropriate temperature gradient along the sample by using our measurement system. Magnetic susceptibility was measured by using a quantum design magnetometer. Several pieces of crystals with the total weight of 2 g were used for specific-heat measurements at temperatures between 0.5 and 70 K using a quasiadiabatic heat-pulse method. The specific-heat data between 0.4 and 300 K were obtained on a disk-shaped sample by using an ac method. The absolute value was determined by the use of the value measured by the quasiadiabatic dc method. The powder x-ray diffraction patterns were recorded at various temperatures from 3 K to 290 K by a rotating-anode diffractometer using Cu K_α radiation. Single-crystal x-ray diffraction measurements were performed with Mo K_α radiation between 50 and 400 K.

Figure 1(a) displays the magnetic susceptibility χ of CeRhAs in a field of 1 T applied along the three principal axes. We note that anisotropy in χ with respect to the field direction is smaller than 10% in the whole temperature range. In addition to a broad maximum centered at $T_\chi=510$ K, one notes three distinct anomalies at $T_1=370$, $T_2=235$, and $T_3=165$ K, respectively, and an upswing below 30 K. The broad maximum is a characteristic of a Ce-based valence-fluctuating system. The decrease of χ in all the di-

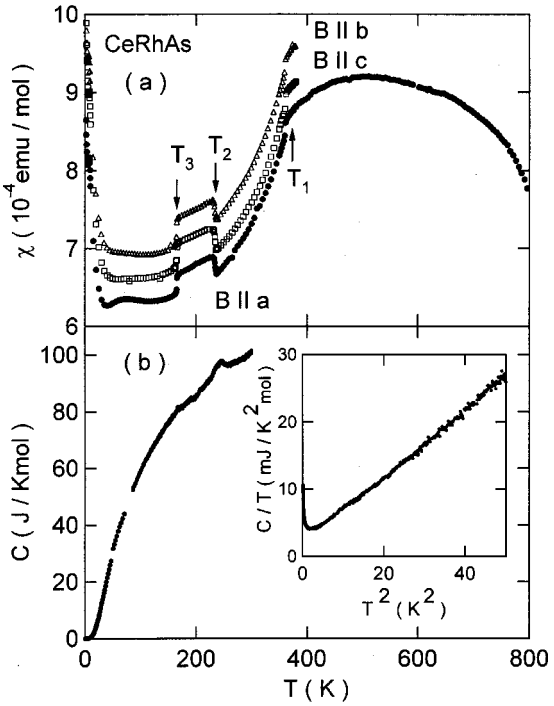

FIG. 1. (a) Temperature dependence of the magnetic susceptibility of single-crystal CeRhAs measured in a field of 1 T applied along the three principal axes. (b) Temperature dependence of the specific heat C. The inset shows C/T vs T^2.

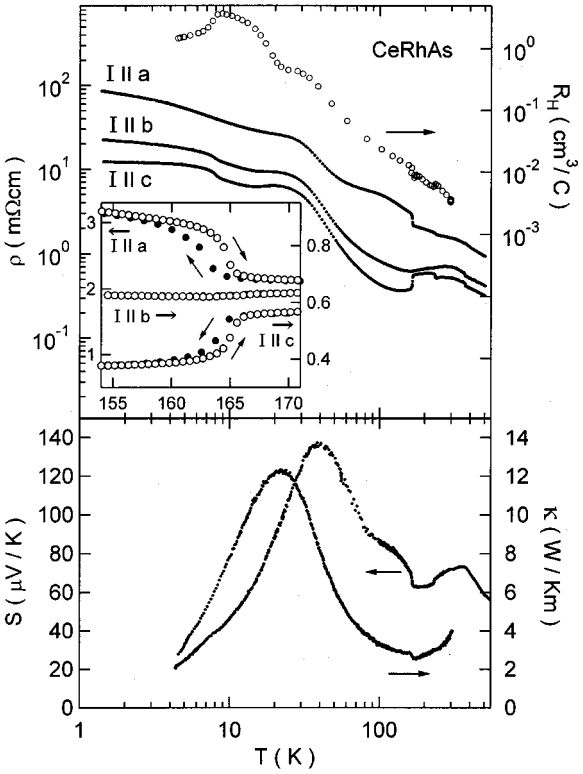

FIG. 2. Temperature dependence of the electrical resistivity, Hall coefficient, thermopower and thermal conductivity for single crystals of CeRhAs. The inset shows the hysteretic behavior of resitivity near the transition at $T_3 = 165$ K.

rections with decreasing temperature from T_1 to 30 K amounts to 30% of the value at the maximum. The abrupt decrease at T_1 indicates the onset of the gap formation in the electronic density of states. For the two steps at T_2 and T_3, neither hysteresis on cooling and heating nor field dependence up to 5 T was observed within the resolution limit of our apparatus. This fact together with the very weak anisotropy may exclude the possibility of ordinary magnetic transitions. Instead, the drop at T_1 and T_3 resembles the type of anomaly one expects from a charge-density wave (CDW) transition[13] or a spin-dimerization transition.[14]

The specific-heat data in Fig. 1(b) possess a hump at around T_2 and a cusp at T_3. This fact confirms that the anomalies at T_2 and T_3 in $\chi(T)$ are associated with some sort of phase transitions. The low-temperature data are replotted as C/T vs T^2 in the inset. We used the fitting functions expressed by $C/T = \gamma + \beta T^2 + \alpha/T^3$, where the last term represents the nuclear quadrupole contribution from the As nucleus in this compound. The fit gives the electronic specific-heat coefficient $\gamma = 3.0$ mJ/K^2 mol. This magnitude suggests the presence of residual density of states at the Fermi level, although the γ value is one order of magnitude smaller than those reported for CeNiSn and CeRhSb, 45 and 20 mJ/K^2 mol, respectively.[15,16] It should be noted that the previous estimation of $\gamma \sim 0$ for a polycrystalline sample was made from a linear extrapolation of the data contaminated with a large peak at 6 K, which originates from an impurity phase with trivalent Ce ions.[10]

Figure 2 displays the temperature dependence of the electrical resistivity ρ, Hall coefficient R_H, thermopower S, and thermal conductivity κ. The ratio $\rho(T = 1.5\ \mathrm{K})/\rho(T = 300\ \mathrm{K})$ is 40–100, being one order of magnitude larger than the value reported for a polycrystalline sample.[10] Three steplike anomalies in $\rho(T)$ are observed at T_1, T_2, and T_3, respectively. An important observation is the strong anisotropy in $\rho(T)$; ρ_a is several times larger and exhibits different behavior than ρ_b and ρ_c. Both ρ_b and ρ_c jump at T_1 while ρ_a jumps at T_3 and ρ_c drops there. As is shown in the inset, hysteretic behavior was observed on cooling and heating through T_3, indicative of a first-order transition. From the activated behavior between 110 and 150 K, the energy gap for ρ_a is estimated to be 282 K, being twice that for ρ_b and ρ_c. The saturated behavior below 20 K is consistent with the presence of residual carriers as inferred from the specific-heat measurement. The significant increase of R_H on cooling from 300 K indicates the steady decrease in the carrier density with a sudden decrease at T_3. The value of R_H at 4.5 K corresponds to a carrier density 1.8×10^{-4}/ f.u. based on the assumption of a single-type of carrier.

The curve of $S(T)$ for an unoriented crystal exhibits a huge maximum of 138 μV/K at 40 K in addition to three anomalies at T_1, T_2, and T_3. The steady increase of $S(T)$ on cooling below T_3 well corresponds to the substantial increase in both $\rho(T)$ and $R_H(T)$ and also to the decrease in $\chi(T)$. These observations suggest the development of the gap in the electronic density of states below T_3. This coincides with the significant enhancement of $\kappa(T)$. Such enhancement of $\kappa(T)$ is attributable to the increase of the phonon contribution to κ.

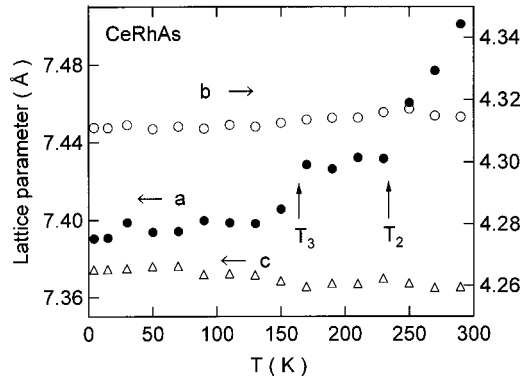

FIG. 3. Temperature dependence of the lattice parameters of CeRhAs determined by powder x-ray diffraction measurements.

It is a consequence of the increase of phonon mean free path due to the reduction of charge carriers as for phonon scatterers.[17] From the knowledge of $\rho(T)$, $S(T)$, and $\kappa(T)$, we evaluate the thermoelectric figure of merit $Z=S^2/\rho\kappa$. If the data of ρ_b are used for $\rho(T)$, Z has a maximum of 1.0 $\times 10^{-3}$ K^{-1} at 120 K, which is comparable with that of the typical valence fluctuating Ce compound $CePd_3$.[9] For the better evaluation of Z, we need to measure $S(T)$ and $\kappa(T)$ along each principal axis.

X-ray powder diffraction patterns of CeRhAs at temperatures from 4 K to 290 K were analyzed by assuming the orthorhombic ε-TiNiSi-type structure.[18] Temperature variations of lattice parameters are plotted in Fig. 3. On cooling, only the *a*-axis parameter strongly decreases with passing through a plateau. The temperatures at the stepwise changes well correspond to T_2 and T_3, respectively, where marked anomalies are manifested in magnetic and transport properties. It should be recalled that in the crystal structure of CeRhAs, the Ce atoms form a zigzag chain along the *a* axis. The shrink along the *a* axis on cooling would enhance the hybridization between Ce $4f$ electron states and the conduction band. In fact, for the isostructural compound CeNiSn, it has been reported that uniaxial-pressure applied along the *a* axis enhances the hybridization and increases the gap magnitude.[19]

In order to study whether the unusual change in the *a*-axis parameter is caused by a structural transformation, we performed single-crystal x-ray diffraction measurements. The result at 290 K revealed that the unit cell is doubled along the *b* and *c* axes. The superlattice reflection at $q_1=(0\ 1/2\ 1/2)$ disappears on heating above T_1, as is shown in Fig. 4. In addition, two types of superlattice peaks grow below T_2, which are described by modulation wave vectors $q_2=(0\ 1/3\ 1/3)$ and $q_3=(1/3\ 0\ 0)$, respectively. The intensity of the satellite peak at q_2 suddenly vanishes below T_3, thereby the other peak at q_3 develops. The stepwise temperature dependence confirms the transition at T_3 to be of the first order, as inferred from the hysteretic behavior in the resistivity. However, the specific-heat data exhibit a rather broad anomaly at around T_3. The broad feature might be due to the temperature cycle that is inevitable for the ac specific-heat measurement.[20] It should be noted that the observed peak intensity for $(+1/3,k,0)$ is much weaker than that for

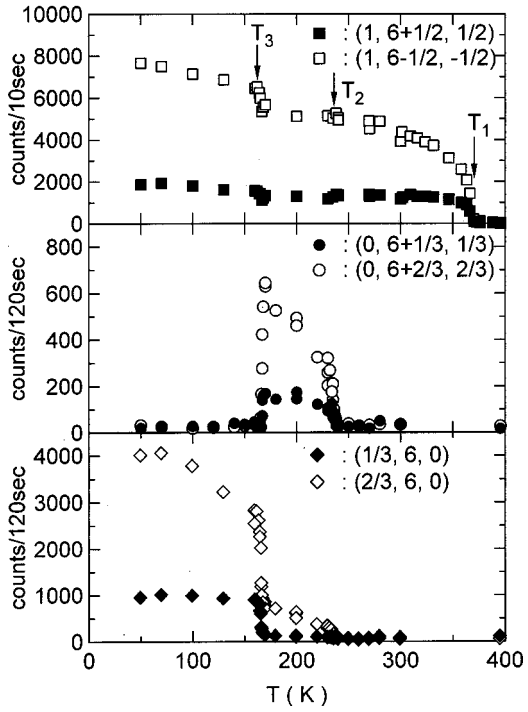

FIG. 4. Temperature dependence of intensities for three sets of satellite reflections of CeRhAs single crystal observed by x-ray diffraction measurements.

$(-1/3,k,0)$, where k is an integer. This asymmetry cannot be explained by taking account of solely the lattice modulation but suggests the modulation of charge density as found in CeP and CeSb, where the layers of Ce ions with two different $4f$-electron orbital states periodically stack along one crystallographic direction.[21]

Let us consider the relation between the superstructures and anomalies observed in bulk properties. The most significant change occurring below $T_1=370$ K is the sudden drop in $\chi(T)$, indicative of the onset of gap formation in the density of states. Thereby, lattice dimerization occurs along the *b* and *c* axes. The jump in ρ_b and ρ_c at T_1 as well as the increase of R_H is consistent with the gap formation. However, photoemission[11] and electron-tunneling[22] measurements suggested the gap opening below T_2 rather than T_1. It should be recalled that these techniques are sensitive to the surface state. If the lattice dimerization is weak on the surface due to strain, then the gap formation temperature may be depressed. In fact, no superlattice peaks were observed by x-ray diffraction measurements on powdered samples at 290 K.

Below T_2, the simultaneous development of two superlattice peaks is reminiscent of the unusual CDW transition in an intermetallic compound $Er_3Ir_4Si_{10}$ with a three-dimensional structure.[23] The Er ions with localized magnetic moments form a chain along the tetragonal *c* axis. Along this direction an incommensurate CDW develops at 155 K, which then locks into a commensurate one below 55 K. For CeRhAs, however, the sudden increase of $\chi(T)$ at T_2 in all the directions is at variance with a CDW transition because the development of CDW's gap over a portion of the Fermi surface

should result in a decrease of $\chi(T)$. Instead, both the increase in $\chi(T)$ and the drop in R_H below T_2 are indicative of suppression of the gap. In Fig. 4, the intensity of superlattice reflection at $q_1=(0\ 1/2\ 1/2)$ stops increasing on cooling from T_2 to T_3 where the lattice modulation with $q_2=(0\ 1/3\ 1/3)$ is present. This fact suggests that the lattice modulation with q_2 interrupts the development of energy gap associated with the lattice modulation with q_1.

Below the first-order transition at T_3, on the other hand, all the anomalies observed in magnetic and transport properties except for the drop in $\rho_c(T)$ are consistent with the further development of energy gap. It should be recalled that threefold modulations along the *b* and *c* axis vanish below T_3. The drop in $\rho_c(T)$ can be explained if the mobility of carriers along the *c* axis is enhanced by the disappearance of the *c*-axis modulation.

The combination of the data of lattice parameter and of satellite peaks indicates that the development of the modulations with q_1 and q_3 results in a significant contraction along the Ce zigzag chain. As a consequence of strong volume dependence of hybridization between the $4f$ states and conduction-electron states, the contraction should promote development of the gap according to the hybridization-gap model.[5] The $4f$ electrons in CeRhAs are in an intermediate-valence state, and they are more strongly hybridized with conduction-electron states compared with the $4f$ electrons in CeNiSn and CeRhSb. It is highly possible that the instability of the $4f$-electron band in CeRhAs drives the structural modulations, which in turn promote the development of the energy gap. To understand this interplay and to examine possible charge ordering, further refinement of crystal structure and studies of electronic states by microscopic techniques are needed.

In conclusion, experimental evidence is provided for three successive phase transitions in the so-called Kondo insulator CeRhAs. To the best of our knowledge, it is the first example of intermediate-valence $4f$ compounds in which superlattice formation is associated with opening of a gap in the density of states. In any events, the close relation between the gap formation and structural modulations urges us to reconsider the model that the local Kondo coupling plays a predominant role in the gap formation.

We thank T. Ekino, M. Udagawa, C. Lee, F. Iga, P. Rogl, and H. Okamura for informative discussion and Y. Shibata for the electron-probe microanalysis. Powder x-ray diffraction measurements were performed at the Cryogenic Center, Hiroshima University. This work was supported in part by a Grant-in Aid for Scientific Research (COE Research 13CE2002) of MEXT, Japan and a NEDO International Joint Research Grant.

[1] G. Aeppli and Z. Fisk, Comments Condens. Matter Phys. **16**, 155 (1992).

[2] T. Takabatake, F. Iga, T. Yoshino, Y. Echizen, K. Katoh, K. Kobayashi, M. Higa, N. Shimizu, Y. Bando, G. Nakamoto, H. Fujii, K. Izawa, T. Suzuki, T. Fujita, M. Sera, M. Hiroi, K. Maezawa, S. Mock, H.v. Löhneysen, A. Brückl, K. Neumaier, and K. Andres, J. Magn. Magn. Mater. **177-181**, 277 (1998).

[3] P.S. Riseborough, Adv. Phys. **49**, 257 (2000).

[4] T. Ekino, T. Takabatake, H. Tanaka, and H. Fujii, Phys. Rev. Lett. **75**, 4262 (1995).

[5] H. Ikeda and K. Miyake, J. Phys. Soc. Jpn. **65**, 1769 (1996).

[6] M.F. Hundley, P.C. Canfield, J.D. Thompson, and Z. Fisk, Phys. Rev. B **50**, 18 142 (1994).

[7] T. Takabatake, H. Tanaka, Y. Bando, H. Fujii, S. Nishigori, T. Suzuki, T. Fujita, and G. Kido, Phys. Rev. B **50**, 623 (1994).

[8] F. Iga, T. Suemitsu, S. Hiura, K. Takagi, K. Umeo, M. Sera, and T. Takabatake, J. Magn. Magn. Mater. **226-230**, 137 (2001).

[9] G.D. Mahan, B. Sales, and J. Sharp, Phys. Today **50** (3), 42 (1997).

[10] S. Yoshii, M. Kasaya, H. Takahashi, and N. Mori, Physica B **223&224**, 421 (1996).

[11] H. Kumigashira, T. Sato, T. Yokota, T. Takahashi, S. Yoshii, and M. Kasaya, Phys. Rev. Lett. **82**, 1943 (1999).

[12] H. Kumigashira, T. Takahashi, S. Yoshii, and M. Kasaya, Phys. Rev. Lett. **87**, 067206 (2001).

[13] D.C. Johnston, Phys. Rev. Lett. **52**, 2049 (1984).

[14] M. Hase, I. Terasaki, and K. Uchinokura, Phys. Rev. Lett. **70**, 3651 (1993).

[15] K. Izawa, T. Suzuki, T. Fujita, T. Takabatake, G. Nakamoto, H. Fujii, and K. Maezawa, Phys. Rev. B **59**, 2599 (1999).

[16] S. Nishigori, H. Goshima, T. Suzuki, T. Fujita, G. Nakamoto, H. Tanaka, T. Takabatake, and H. Fujii, J. Phys. Soc. Jpn. **65**, 2614 (1996).

[17] Y. Isikawa, K. Mori, Y. Ogiso, K. Oyabe, and K. Sato, J. Phys. Soc. Jpn. **60**, 2514 (1991).

[18] P. Salamakha, O. Sologub, T. Suemitsu, and T. Takabatake, J. Alloys Compd. **313**, L5 (2000).

[19] K. Umeo, T. Igaue, H. Chyono, Y. Echizen, T. Takabatake, M. Kosaka, and Y. Uwatoko, Phys. Rev. B **60**, R6957 (1999).

[20] D.T. Adroja, Y. Echizen, T. Takabatake, Y. Matsumoto, T. Suzuki, T. Fujita, and B.D. Rainford, J. Phys.: Condens. Matter **11**, 543 (1999).

[21] K. Iwasa, A. Hannan, M. Kohgi, and T. Suzuki, Phys. Rev. Lett. **88**, 207201 (2002).

[22] T. Ekino, T. Takasaki, T. Suemitsu, T. Takabatake, and H. Fujii, Physica B (to be published).

[23] F. Galli, S. Ramakrishnan, T. Taniguchi, G.J. Nieuwenhuys, J.A. Mydosh, S. Geupel, J. Ludecke, and S. van Smaalen, Phys. Rev. Lett. **85**, 158 (2000).